Regional incision of the eastern margin of the Tibetan Plateau

William Ouimet[1], Kelin Whipple[2], Leigh Royden[3], Peter Reiners[4], Kip Hodges[2], and Malcolm Pringle[3]
[1]DEPARTMENT OF GEOLOGY, AMHERST COLLEGE, AMHERST, MASSACHUSETTS 01002, USA
[2]SCHOOL OF EARTH AND SPACE EXPLORATION, ARIZONA STATE UNIVERSITY, TEMPE, ARIZONA 85287, USA
[3]DEPARTMENT OF EARTH, ATMOSPHERIC, AND PLANETARY SCIENCES, MASSACHUSETTS INSTITUTE OF TECHNOLOGY, CAMBRIDGE, MASSACHUSETTS 02139, USA
[4]DEPARTMENT OF GEOSCIENCES, UNIVERSITY OF ARIZONA, TUCSON, ARIZONA 85721, USA

ABSTRACT

New (U-Th)/He analyses from three elevation transects collected within river gorges that dissect the eastern margin of the Tibetan Plateau provide constraints on the rates and timing of accelerated river incision into the high-elevation, low-relief topography of the region. Apatite He data from the easternmost transect (Dadu River), ~120 km from the plateau margin adjacent to the Sichuan Basin, indicate that rapid river incision of ~0.33 ± 0.04 km/m.y. began at ca. 10 Ma and has continued to the present. Apatite He and zircon He data from the middle transect (Yalong River), collected ~225 km SSW of the Dadu data, indicate that rapid river incision of ~0.34 ± 0.02 km/m.y. began prior to ca. 14 Ma and continued until the early Quaternary, when it increased, likely in response to local uplift and erosion associated with active faults nearby. Apatite He and zircon He data from the westernmost transect (Yangtze River), ~210 km W of the Yalong data, indicate that rapid river incision of ~0.38 ± 0.04 km/m.y. began at or prior to ca. 10 Ma, though likely not prior to ca. 15 Ma, and has continued to the present. The regional consistency of these data indicates that the entire eastern margin of the Tibetan Plateau was being dissected by 10 Ma and that incision has been relatively constant and uniform in the region since that time; this pattern is consistent with an erosional response to broad regional uplift at or before 10 Ma. The larger amount, and earlier onset, of exhumation observed in the Yalong River gorge shows that certain areas on the eastern margin deviate from a simple regional pattern of epeirogenic uplift and subsequent river incision and probably reflect the superposition of local upper-crustal deformation and uplift on the broad regional pattern.

LITHOSPHERE; v. 2; no. 1; p. 50–63. doi: 10.1130/L57.1

INTRODUCTION

An understanding of the rates and spatial patterns of erosion is crucial for studying the shape and evolution of mountainous landscapes. On the eastern margin of the Tibetan Plateau, major rivers have locally cut deep gorges 2–3 km deep into regionally elevated, low-relief, relict topography that represents the landscape that existed throughout the eastern margin prior to regional uplift and subsequent incision (Clark et al., 2006) (Fig. 1). The incision and evolution of these river gorges dictate the style and pace of all landscape adjustment in response to regional plateau uplift and local tectonic deformation. In this paper, we explore new constraints on long-term erosion rates and the initiation age of accelerated river incision in three river gorges dissecting the eastern margin using apatite and zircon (U-Th)/He thermochronometry. The purpose of this study is twofold: (1) to test and refine the hypothesis that uplift and subsequent incision into slowly eroding, relict topography on the eastern margin began between 9 and 13 Ma and that it was regional (i.e., Clark et al., 2005); and (2) to better quantify long-term erosion rates associated with major rivers dissecting the eastern margin. Our approach is to focus on elevation transects collected over short horizontal distances (<5 km) in each of the Dadu, Yalong, and Yangtze River gorges (Fig. 1). In addition to providing important estimates of local long-term erosion rates and the initiation of river incision, these transects are important for constraining geodynamic models that explore the late Cenozoic evolution of the eastern margin of the Tibetan Plateau.

Background

The eastern margin of the Tibetan Plateau contains a wide range of bedrock lithologies deformed in the assembly of Eurasia (e.g., Dirks et al., 1994; Burchfiel et al., 1995; Chen et al., 1995; Chen and Wilson, 1996) (Fig. 2). Cooling ages from high-temperature thermochronology (>300 °C) in granites scattered throughout the eastern margin are typically older than 50 Ma, reflecting either Triassic-Jurassic crystallization ages or slow cooling of those granites from the late Mesozoic up to the middle Cenozoic (Wallis et al., 2003; Roger et al., 2004; Reid et al., 2005). Cooling ages from low-temperature thermochronology (<200 °C) from the same (or similar aged) granites, meanwhile, vary substantially (from older than 100 Ma to younger than 5 Ma), reflecting either the older, slowly cooling relict topography, or late Cenozoic tectonic activity, uplift, exhumation, and river incision driven by deformation associated with the India-Asia collision (Arne et al., 1997; Xu and Kamp, 2000; Kirby et al., 2002; Clark et al., 2005; Qingzhou et al., 2007; Kirby, 2008; Godard et al., 2009). The only area known to have experienced enough exhumation to display young ages for both high- and low-temperature thermochronometers occurs in the vicinity of Gongga Shan (7556 m; GS in figure maps), within an ~600 km^2 area that deviates from regional characteristics in terms of having higher peak elevations and extremely rugged, intensely glaciated topography. Rapid exhumation in the Gongga Shan area began ca. 12 Ma (Roger et al., 1995; Niemi et al., 2003), and evidence here shows the highest short-term (10^2–10^5 yr) erosion rates in the region (>1–2 mm/yr), measured with cosmogenic nuclides (Ouimet et al., 2009).

Using regionally distributed age-elevation data and multiple thermochronometers, the onset of accelerated exhumation in the region has been constrained to between 8 and 12 Ma for the Longmen Shan and Min River area north of the Sichuan Basin (Kirby et al., 2002; Kirby, 2008; Godard et al., 2009), and between 9 and 13 Ma for the Dadu and Yalong River gorges incised into the plateau interior (Clark et al., 2005). These data yield estimates of long-term (10^6–10^7 yr), late Cenozoic erosion rates for

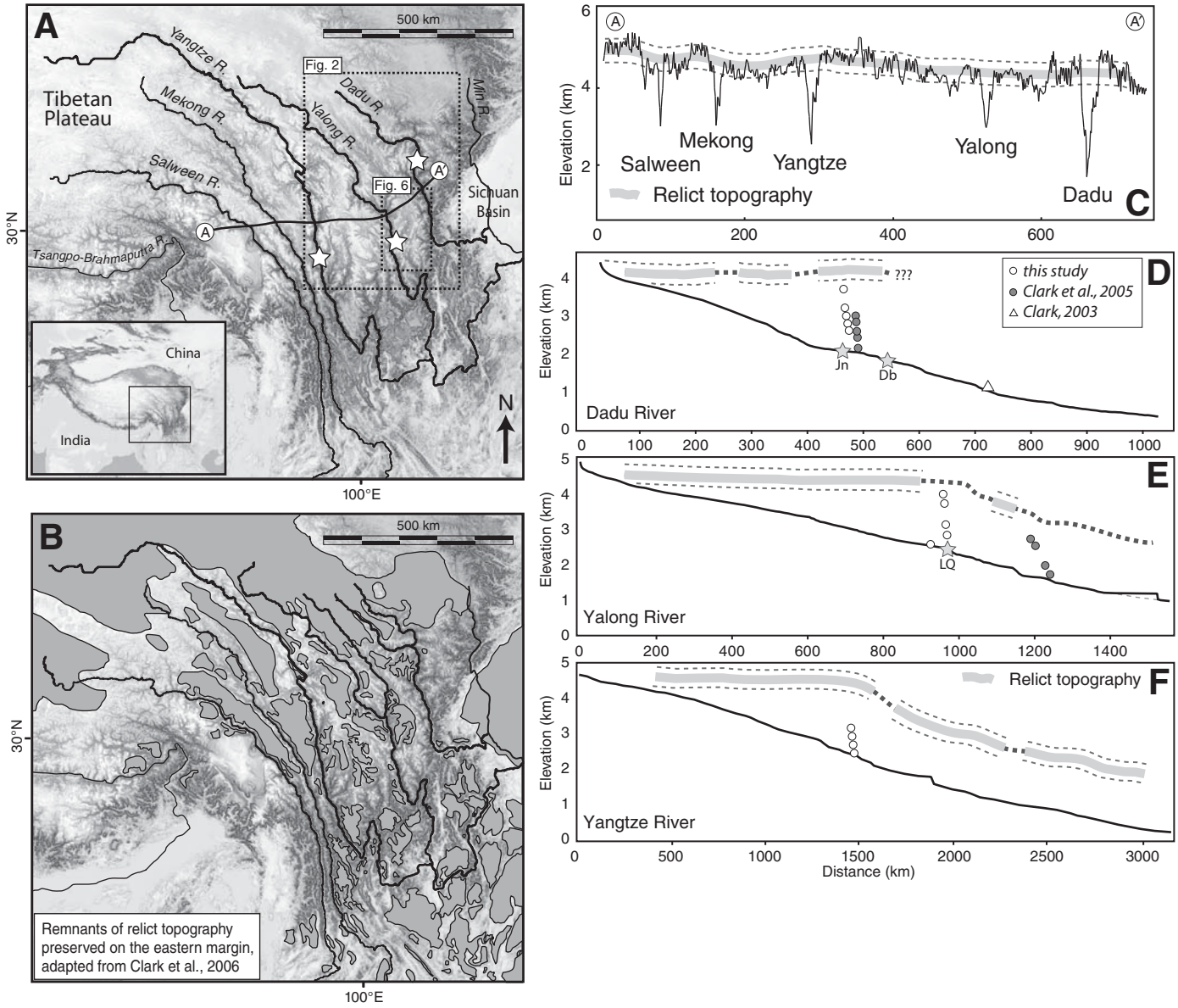

Figure 1. Regional topography and rivers. (A) Overview map of regional topography and rivers of the eastern margin of the Tibetan Plateau. Sample transect locations for this study are indicated by white stars. (B) Patches of low-relief, relict landscape preserved at high elevations. For a detailed description of the criterion used to identify patches of relict landscape, see Clark et al. (2006). (C) Topographic cross section (path A to A′ indicated in A), extracted from the ~1 km resolution GTOPO30 digital elevation model. (D–F) Longitudinal profiles of the Dadu, Yalong, and Yangtze Rivers extracted from 90 m Shuttle Radar Topography Mission (SRTM) data with transect sample locations indicated. For each major river, we also plot projections of the relict topography above the modern river level (for a map of relict topography remnants, elevations, and details of associated interpolation, see Clark et al., 2006). Bold light-gray lines indicate well-preserved remnants of relict topography within 30 km of the river gorges; the typical ±500 m relief for relict topography is indicated by dashed gray lines. Dashed, bold gray lines indicate interpolated relict topography. Note: horizontal scale is different for each profile. Stars indicate the locations of towns Danba (Db) and Jinchuan (Jn) on the Dadu River profile, and the confluence of the Li Qui River (LQ) with the Yalong trunk river on the Yalong River profile.

the Dadu and Yalong River gorges on the order of 0.25–0.5 mm/yr, and 0.5–1 mm/yr for the Longmen Shan. Clark et al. (2005) used the remnants of relict topography and an interpolation of relict topography, where it was missing, to measure the depth of samples below the low-relief landscape. This resulted in a pseudo–age-elevation (or age-depth) relationship that exhibited an inflection point bracketing the initiation of rapid long-term erosion rate. No single transect, however, contained the right combination of ages and elevations (or depth of incision) to capture the exact timing of accelerated incision, nor to directly record the inferred acceleration.

As discussed by Clark et al. (2006), the reconstructed regional low-relief surface constrains the total amount and pattern of regional uplift where the relict low-relief surface is preserved (Fig. 1). Locally higher, glaciated areas preserve no record of this low-relief surface and may either reflect initial topographic highs, areas of more extensive erosion, or areas of greater late Cenozoic uplift. There are no data for the eastern margin of the plateau that directly constrain the timing of uplift. Uplift must have been contemporaneous with, or predated, river incision (Schoenbohm et al., 2004; Clark et al., 2006). A significant lag time between uplift and

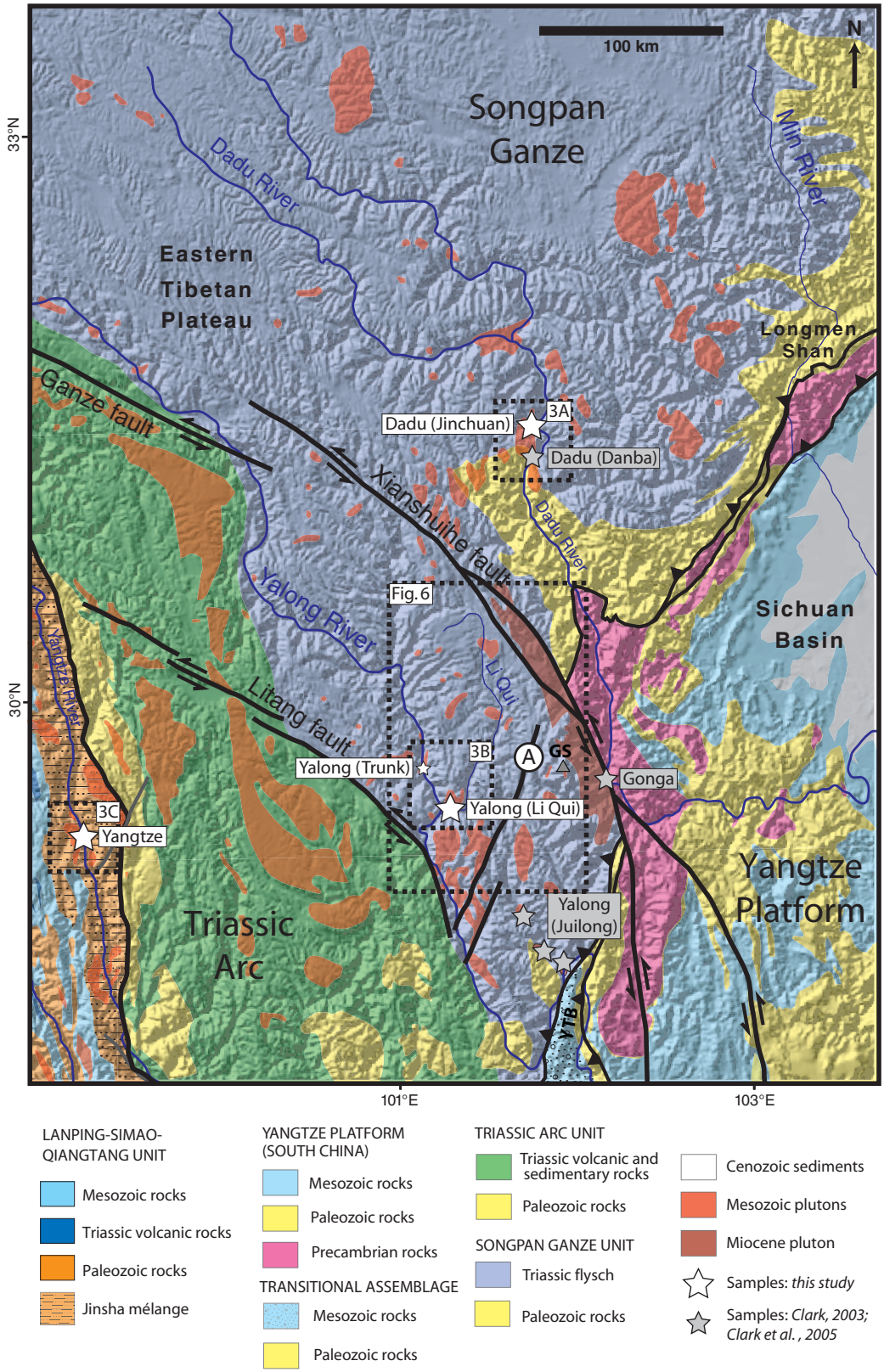

Figure 2. Regional geologic map. Tectonic and geologic map of the study area, adapted from B. Clark Burchfiel (2009, personal commun.) and *Geologic Map of the Tibetan Plateau and Adjacent Areas* compiled by Chengdu Institute of Geology and Mineral Resources and Chinese Geological Survey (map scale 1:1,500,000). Sample transect locations for this study are indicated by white stars. Each granite sampled is mapped as a Mesozoic pluton. Gray stars indicate the location of data from Clark (2003) and Clark et al. (2005). Dashed boxes indicate the close-up maps in Figures 3A, 3B, and 3C and topography in Figure 6. Location "A" marks the fault discussed in the text. GS—Gongga Shan. YBT—Yalong thrust belt.

incision is possible if river incision was particularly inefficient, such as in hyperarid conditions or areas with very low gravel flux (e.g., Whipple, 2004; Pelletier, 2007). Previous workers have argued that such lag times were probably short (<2 m.y.) in the region, particularly along the very steep Longmen Shan margin, and thus have taken the timing of river incision as a proxy for the timing of regional uplift (Kirby et al., 2002; Schoenbohm et al., 2004, Clark et al., 2006). However, our understanding of transient river response to uplift and climate change is sufficiently incomplete that we must entertain the possibility of a significant lag time. Any such lag time would presumably vary with distance upstream on major rivers (e.g., Whipple and Tucker, 1999), and indeed the widespread preservation of a relict low-relief upland indicates that the incision signal has yet to propagate up smaller tributaries. Incision amounts, and therefore plausibly the duration of rapid incision, clearly decrease upstream from our sample transects in all three major rivers (Fig. 1). We build on the earlier work by testing the hypothesis of synchronous regional uplift and incision and also by refining estimates of the rates and timing of accelerated river incision into the high topography of the region. The goal is to build a better picture of regional long-term erosion rates, as well as provide tighter constraints on incision for the other major rivers. The pattern and rates of the propagation of river incision upstream along rivers are discussed in more detail by Ouimet (2007) and will be explored further in future papers.

METHODS

Similar to previous thermochronologic work on the eastern margin, we use low-temperature thermochronology to explore the incision history of major river gorges. We focus on (U-Th)/He thermochronometry in apatites (AHe) and zircons (ZHe), which reflect rock cooling and simple exhumation through the ~70 °C and ~180 °C isotherms, respectively (Farley, 2000; Reiners et al., 2004). Assuming a geothermal gradient of 30–40 °C/km, the respective closure isotherms for AHe and ZHe are ~1.5–2 km and ~4.3–5.7 km beneath the surface. On the eastern margin, river gorges typically have maximum depths of only 2–3 km beneath the regionally preserved, low-relief relict topographic surface (Fig. 1), suggesting that AHe is best suited for studying the young incision of these gorges. We utilized the age-elevation method to determine rates of bedrock cooling in river gorges, which allows for estimates of erosion rate to be made independently of assumptions about the geothermal gradient.

Samples collected along steep topographic profiles are considered equivalent to sampling at depth beneath Earth's surface, thus yielding an age-elevation relationship that can be interpreted as the velocity of rocks relative to the closure isotherm (i.e., erosion rate) at the time of closure (e.g., Wagner and Reimer, 1972). The important assumptions of this method include: (1) the closure isotherm was horizontal (relative to samples) at the time of closure, and exhumation is vertical; (2) the geothermal gradient and surface temperature have remained constant through time, such that the depth of the closure isotherm has remained constant relative to the surface; (3) samples have experienced a spatially uniform erosion rate (i.e., the transect does not cross any active structures); and (4) there has been no deformation or offset of the samples. The influence of topography on closure isotherm geometry complicates the interpretation of age-elevation in terms of absolute long-term erosion rates (Stuwe et al., 1994; Mancktelow and Grasemann, 1997; Braun, 2005; Ehlers, 2005). For this reason, we discuss all erosion rates derived from age-elevation data as apparent erosion rates, acknowledging that absolute erosion rates depend on the kinematics of eroding, evolving surface topography, and closure isotherms.

Sample Transects

We collected samples for age-elevation analysis over short horizontal distances (<5 km) to limit the influence of topography on estimated erosion rates (Table 1; Fig. 3). Samples for all three transects came from Mesozoic granitic intrusions that outcrop within the Dadu, Yalong, and Yangtze River gorges (Roger et al., 2004; Reid et al., 2005) (Fig. 2). The granitic bodies sampled for the Dadu and Yalong transects intrude the folded and faulted Songpan-Ganze flysch terrane containing metamorphosed sandstone and mudstone beds of variable thickness; the granitic body sampled for the Yangtze transect intrudes Paleozoic sediments of the Jinsha mélange between the Qiangtang block and Triassic Yidun Arc in westernmost Sichuan (Fig. 2). The Dadu granite is undeformed; the Yalong and Yangtze granites are deformed and foliated.

Samples from the three transects were crushed, and aliquots rich in apatite and zircon were prepared using standard heavy liquid and magnetic techniques. Fourteen samples yielded apatites of sufficient quality for analysis. Final separates for (U-Th)/He analyses were hand-picked using a 100x microscope to ensure purity and selected for euhedral shape, appropriate size, and absence of inclusions. Separates were then wrapped in Pt (apatite) and Nb (zircon) foils. He abundances for each crystal were measured by laser mass spectrometry (for methods, see Reiners, 2003), and U and Th concentrations were measured by isotope dilution. An α-ejection correction (*Ft*) was applied to each crystal analysis to derive a corrected (U-Th)/He age (Farley, 2000; Reiners, 2005).

TABLE 1. SAMPLE DESCRIPTIONS

Transect	Sample ID	Rock type	Age	Long. (°N)	Lat. (°E)	Elev. (m)	Apatite replicates	Zircon replicates
Dadu (Jinchuan)	wbo-04-32C	Granite	Mz	101.9127	31.3871	3700	2	–
Dadu (Jinchuan)	wbo-03-20B	Granite	Mz	101.9211	31.3780	3200	4	–
Dadu (Jinchuan)	wbo-03-20C	Granite	Mz	101.9256	31.3740	3000	4	–
Dadu (Jinchuan)	wbo-03-20D	Granite	Mz	101.9361	31.3708	2800	2	–
Dadu (Jinchuan)	wbo-03-20E	Granite	Mz	101.9418	31.3711	2600	4	–
Yalong (Li Qui)	wbo-04-41C	Granite	Mz	101.2441	29.4602	4000	4	2
Yalong (Li Qui)	wbo-04-41A	Granite	Mz	101.2402	29.4479	3700	4	1
Yalong (Li Qui)	wbo-03-16A	Granite	Mz	101.2354	29.4315	3100	2	–
Yalong (Li Qui)	wbo-04-41E	Granite	Mz	101.2275	29.4203	2800	3	4
Yalong (Trunk)	wbo-04-19	Granite	Mz	101.0830	29.6696	2500	1	–
Yangtze	wbo-04-15	Granite	Mz	99.0728	29.4840	3100	4	4
Yangtze	wbo-04-14	Granite	Mz	99.0698	29.4822	2900	3	–
Yangtze	wbo-04-13	Granite	Mz	99.0682	29.4798	2700	4	3
Yangtze	wbo-04-10	Granite	Mz	99.0612	29.4142	2350	2	3

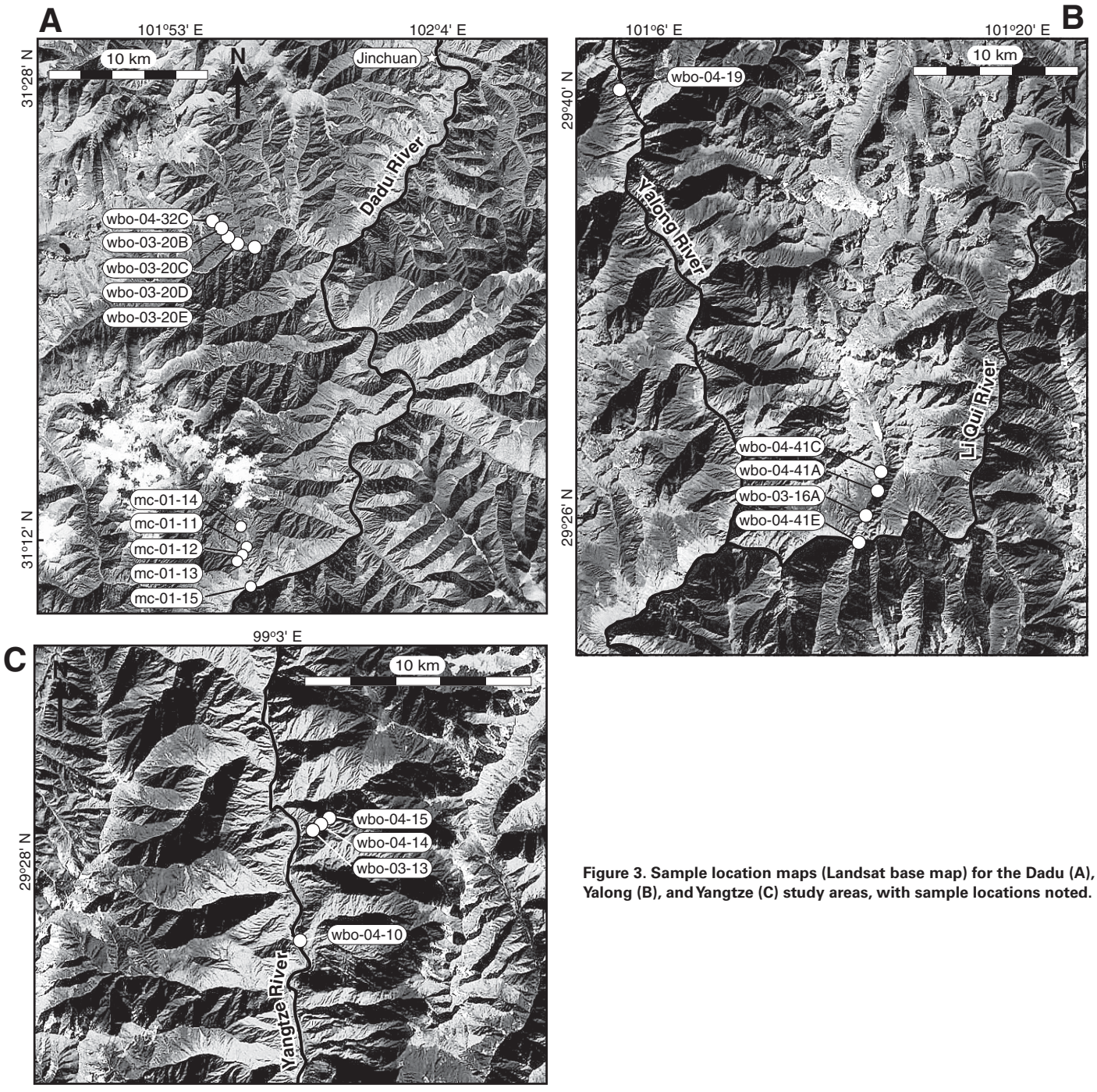

Figure 3. Sample location maps (Landsat base map) for the Dadu (A), Yalong (B), and Yangtze (C) study areas, with sample locations noted.

APATITE AND ZIRCON He RESULTS

A summary of all individual and mean AHe and ZHe analyses is presented in Tables 2, 3, and 4. We report (U-Th)/He ages for five samples from the Dadu transect, five from the Yalong, and four from the Yangtze that cover the full range of elevations for each transect and yield apatite and zircon grains suitable for analysis. All 14 of these samples were analyzed for single-grain apatite (U-Th)/He ages (AHe); only six were analyzed for single-grain zircon (U-Th)/He ages (ZHe) (Tables 2 and 3). All samples run for AHe have more than one single-grain analysis (except for wbo-04-19); all samples run for ZHe have more than one single-grain analysis (except for wbo-04-41A). Errors on the (U-Th)/He ages (2σ) are based on analytical uncertainty in U, Th, and He measurements. For all samples with multiple replicates, we calculated a mean and standard deviation for the spread of replicate analyses (Table 4). We identified six AHe ages as outliers (with ages far from the rest of the replicates for that sample) and excluded them from mean calculations. Grains may end up as outliers for a number of reasons, including the presence of small inclusions rich in U or Th, severe systematic zoning of U or Th, uncertainty in the α-ejection correction, or He implantation from

TABLE 2. APATITE (U-Th)/He INDIVIDUAL CRYSTAL DATA

Transect	Sample replicate	Mass (μg)	Radius (μm)	[U] (ppm)	[Th] (ppm)	[Sm] (ppm)	[4He] (nmol/g)	Ft	Corrected age* (Ma)	2σ† (Ma)
Dadu (Jinchuan)	wbo-04-32CaA	0.96	34.8	43.0	4.9	268	5.46	0.63	36.1	1.69
Dadu (Jinchuan)	wbo-04-32CaB	0.90	38.4	53.2	1.6	332	3.60	0.64	19.3	0.86
Dadu (Jinchuan)	wbo-03-20BaA	0.66	32.3	15.2	5.7	324	1.14	0.59	21.0	1.00
Dadu (Jinchuan)	wbo-03-20BaB	1.41	38.0	13.9	6.5	309	0.84	0.66	14.9	0.67
Dadu (Jinchuan)	wbo-03-20Ba1	1.28	32.3	30.2	14.7	301	1.72	0.62	15.0	1.07
Dadu (Jinchuan)	wbo-03-20Ba2	1.67	41.0	18.4	4.3	188	1.06	0.69	14.4	0.76
Dadu (Jinchuan)	wbo-03-20CaA	1.86	35.8	30.1	10.6	181	0.83	0.66	7.1	0.31
Dadu (Jinchuan)	wbo-03-20CaB	0.92	32.8	53.4	17.0	340	1.77	0.62	9.2	0.38
Dadu (Jinchuan)	wbo-03-20Ca1	1.33	43.5	35.7	27.7	138	1.04	0.67	6.8	0.32
Dadu (Jinchuan)	wbo-03-20Ca2	0.94	31.0	67.2	23.2	273	2.31	0.61	9.7	0.47
Dadu (Jinchuan)	wbo-03-20Da1	0.68	31.0	25.0	19.5	313	0.87	0.55	9.7	0.61
Dadu (Jinchuan)	wbo-03-20Da2	1.95	41.5	25.8	6.6	316	0.73	0.69	7.1	0.37
Dadu (Jinchuan)	wbo-03-20EaA	3.87	52.9	13.2	10.8	273	0.75	0.75	11.6	0.43
Dadu (Jinchuan)	wbo-03-20EaB	1.49	36.8	18.5	16.7	306	0.55	0.65	6.9	0.30
Dadu (Jinchuan)	wbo-03-20Ea1	3.71	50.0	6.7	4.5	280	0.80	0.74	***25.0***	1.31
Dadu (Jinchuan)	wbo-03-20Ea2	0.77	34.5	33.8	45.6	372	0.97	0.62	6.4	0.38
Yalong (Li Qui)	wbo-04-41CaA	4.55	58.1	62.8	29.8	97	1.53	0.77	5.3	0.20
Yalong (Li Qui)	wbo-04-41CaB	2.69	46.9	23.8	23.0	90	0.76	0.72	6.7	0.26
Yalong (Li Qui)	wbo-04-41Ca1	4.17	51.3	74.2	30.6	73	1.61	0.75	4.9	0.21
Yalong (Li Qui)	wbo-04-41Ca2	4.58	60.0	66.6	31.8	78	1.69	0.77	5.5	0.24
Yalong (Li Qui)	wbo-04-41AaA	2.10	39.8	36.3	16.5	117	0.68	0.68	4.6	0.19
Yalong (Li Qui)	wbo-04-41AaB	1.77	38.7	54.1	16.3	143	1.51	0.67	***7.1***	0.29
Yalong (Li Qui)	wbo-04-41Aa1	1.43	34.0	39.5	9.1	105	0.69	0.62	4.9	0.24
Yalong (Li Qui)	wbo-04-41Aa2	2.17	40.3	45.4	10.7	124	0.79	0.67	4.6	0.21
Yalong (Li Qui)	wbo-03-16AaA	1.37	34.4	25.5	6.3	528	0.38	0.64	3.9	0.19
Yalong (Li Qui)	wbo-03-16AaB	1.32	39.6	22.2	5.5	315	0.28	0.67	3.3	0.20
Yalong (Li Qui)	wbo-04-41EaA	0.92	33.5	4.9	5.0	179	0.04	0.61	2.2	0.89
Yalong (Li Qui)	wbo-04-41Ea1	0.75	32.8	9.3	3.5	484	0.06	0.60	1.7	0.72
Yalong (Li Qui)	wbo-04-41Ea2	4.27	51.8	38.6	16.3	507	0.20	0.75	1.2	0.06
Yalong (Trunk)	wbo-04-19aA	1.19	33.1	41.1	52.3	258	0.43	0.62	2.4	0.13
Yangtze	wbo-04-15aA	1.21	34.9	39.0	24.8	144	1.51	0.64	9.8	0.41
Yangtze	wbo-04-15aB	1.08	31.7	43.4	31.6	185	1.44	0.61	8.6	0.38
Yangtze	wbo-04-15a1	1.09	35.0	58.2	23.0	172	1.76	0.61	8.4	0.37
Yangtze	wbo-04-15a2	1.00	31.8	62.5	24.4	177	2.04	0.59	9.3	0.43
Yangtze	wbo-04-14a1	2.57	42.3	51.5	12.8	156	1.57	0.69	7.7	0.34
Yangtze	wbo-04-14a2	4.70	46.8	51.4	12.8	153	2.11	0.73	9.9	0.42
Yangtze	wbo-04-14aB	0.83	35.0	60.4	13.6	186	7.21	0.62	***33.7***	1.37
Yangtze	wbo-04-13aA	2.47	42.7	60.2	7.6	216	2.14	0.71	9.1	0.38
Yangtze	wbo-04-13aB	1.20	36.5	89.3	14.9	227	4.74	0.65	***14.5***	0.60
Yangtze	wbo-04-13a1	3.26	46.3	54.1	3.6	176	1.42	0.73	6.6	0.30
Yangtze	wbo-04-13a2	1.21	36.0	51.1	1.0	184	1.95	0.66	***10.7***	0.54
Yangtze	wbo-04-10aA	0.90	31.5	19.2	23.7	164	0.59	0.60	7.3	0.35
Yangtze	wbo-04-10aB	1.65	38.4	14.8	24.1	150	0.52	0.66	7.1	0.33

Note: Ft—alpha-ejection correction factor (i.e., bulk retentivity).
*Alpha-ejection corrected ages; bold-italic ages are outliers, which are not plotted in results and are excluded in mean calculations.
†Error includes analytical precision only.

adjacent crystals in the host rock. These attributes may also account for the variability in replicate analyses.

Dadu River

We refer to our data from the Dadu River gorge as the Dadu (Jinchuan) transect. This transect was collected in a side tributary to the Dadu River 17 km south of the town of Jinchuan in Maerkang County (Sichuan) (Fig. 3A). At the tributary junction, the Dadu River is 2100 m in elevation. Our sample transect starts 6 km up the side tributary at an elevation of 2600 m. The five samples within the transect ranged in elevation from 2600 m to 3700 m and were collected over a horizontal distance of 3.4 km. The AHe ages for these samples range from 6.4 ± 0.4 Ma to 36.1 ± 1.7 Ma (Fig. 4A; Table 2). We did not analyze ZHe for this transect. We include data from Clark et al. (2005) in our analysis of the Dadu (Danba) transect. The Dadu (Danba) transect data in Clark et al. (2005) was collected 20 km south within the same Mesozoic granitic pluton as our Dadu (Jinchuan) transect. The elevation range of their Dadu (Danba) data is 2100–3000 m; mean AHe ages range from 5.5 ± 0.3 Ma to 9.4 ± 1.7 Ma. The two data sets exhibit similar AHe age-elevation relationships below 3000 m (Fig. 4A). The AHe age-elevation data in our new Dadu (Jinchuan) transect clearly exhibit a break in slope at ca. 10 Ma.

Yalong River

We refer to our data from the Yalong River gorge as the Yalong (Li Qui) transect. The Li Qui River is a large tributary to the Yalong that runs through Xinduqiao ~50 km west of Kangding in western Sichuan.

TABLE 3. ZIRCON (U-Th)/He INDIVIDUAL CRYSTAL DATA

Transect	Sample replicate	Mass (mg)	Radius (mm)	[U] (ppm)	[Th] (ppm)	U/Th	[4He] (nmol/g)	Ft	Corrected age* (Ma)	2σ† (Ma)
Yalong (Li Qui)	WBO-04-41CzC	42.9	79.3	1385	558	2.48	100	0.87	14.0	0.63
Yalong (Li Qui)	WBO-04-41CzD	19.3	61.3	2373	830	2.86	155	0.84	13.4	0.60
Yalong (Li Qui)	WBO-04-41AzA	11.2	46.4	1020	128	7.98	53	0.80	11.7	0.65
Yalong (Li Qui)	WBO-04-41EzA	10.4	48.6	6991	942	7.42	273	0.80	8.7	0.46
Yalong (Li Qui)	WBO-04-41EzC	21.0	59.8	1391	403	3.46	65	0.84	9.7	0.51
Yalong (Li Qui)	WBO-04-41EzD	21.0	59.8	4014	411	9.77	154	0.84	8.3	0.39
Yalong (Li Qui)	WBO-04-41EzE	20.0	55.8	7931	3670	2.16	303	0.83	7.7	0.34
Yangtze	WBO-04-15zA	9.8	48.5	1544	174	8.85	324	0.80	47.2	2.51
Yangtze	WBO-04-15zB	5.1	41.8	1421	253	5.62	160	0.77	26.1	1.40
Yangtze	WBO-04-15zC	9.1	42.8	4099	616	6.65	293	0.78	16.3	0.77
Yangtze	WBO-04-15zD	4.9	39.3	1663	290	5.74	301	0.76	42.5	1.97
Yangtze	WBO-04-13zA	7.9	46.8	533	171	3.11	56	0.79	23.0	0.95
Yangtze	WBO-04-13zB	8.6	49.0	713	245	2.91	70	0.80	21.1	0.86
Yangtze	WBO-04-13zC	3.9	40.8	1029	378	2.72	101	0.75	22.4	0.93
Yangtze	WBO-04-10zA	6.0	48.8	2343	502	4.67	299	0.79	28.6	1.51
Yangtze	WBO-04-10zC	5.5	41.5	1031	307	3.36	192	0.77	42.0	1.72
Yangtze	WBO-04-10zD	4.2	47.5	1715	252	6.80	502	0.77	68.2	2.96

Note: Ft—alpha-ejection correction factor (i.e., bulk retentivity).
*Alpha-ejection corrected ages.
†Error includes analytical precision only.

TABLE 4. (U-Th)/He MEAN AGES

Transect	Sample ID	Elevation (m)	Mean age apatite (Ma)	Mean age zircon (Ma)	Reference
Dadu (Jinchuan)	WBO-04-32C	3700	27.7 ± 11.9	– ± –	This study
Dadu (Jinchuan)	WBO-03-20B	3200	16.3 ± 3.1	– ± –	This study
Dadu (Jinchuan)	WBO-03-20C	3000	8.2 ± 1.5	– ± –	This study
Dadu (Jinchuan)	WBO-03-20D	2800	8.4 ± 1.9	– ± –	This study
Dadu (Jinchuan)	WBO-03-20E	2600	6.6 ± 0.3	– ± –	This study
Yalong (Li Qui)	WBO-04-41C	4000	5.6 ± 0.8	13.7 ± 0.5	This study
Yalong (Li Qui)	WBO-04-41A	3700	4.7 ± 0.2	11.7 ± 0.7	This study
Yalong (Li Qui)	WBO-03-16A	3100	3.6 ± 0.5	– ± –	This study
Yalong (Li Qui)	WBO-04-41E	2800	1.7 ± 0.5	8.6 ± 0.8	This study
Yangtze	WBO-04-15	3100	9.0 ± 0.7	33.0 ± 14.3	This study
Yangtze	WBO-04-14	2900	8.8 ± 1.5	– ± –	This study
Yangtze	WBO-04-13	2700	7.8 ± 1.8	22.2 ± 1.0	This study
Yangtze	WBO-04-10	2350	7.2 ± 0.1	46.3 ± 20.2	This study
Dadu (Danba)	MC-01-11	2840	8.1 ± 1.2	– ± –	Clark et al. (2005)
Dadu (Danba)	MC-01-12	2580	6.1 ± 0.5	– ± –	Clark et al. (2005)
Dadu (Danba)	MC-01-13	2500	5.7 ± 0.1	– ± –	Clark et al. (2005)
Dadu (Danba)	MC-01-14	3000	9.4 ± 1.7	– ± –	Clark et al. (2005)
Dadu (Danba)	MC-01-15	2100	5.5 ± 0.3	– ± –	Clark et al. (2005)
Yalong (Juilong)	MC-01-25	1700	4.6 ± 1.1	– ± –	Clark et al. (2005)
Yalong (Juilong)	MC-01-27	1950	5.0 ± 1.7	– ± –	Clark et al. (2005)
Yalong (Juilong)	MC-01-29	2550	8.3 ± 2.8	– ± –	Clark et al. (2005)
Yalong (Juilong)	MC-01-30	2750	10.1 ± 7.8	– ± –	Clark et al. (2005)
Gongga	MC-01-07	1150	0.42 ± 0.38	– ± –	Clark (2003)

Our Yalong (Li Qui) transect was collected adjacent to the lower Li Qui River, 10 km upstream from the confluence of the Li Qui with the Yalong (Fig. 3B). At the confluence, the Yalong is ~2400 m in elevation. The four samples within the main transect ranged in elevation from 2800 m to 4000 m and were collected over a horizontal distance of 4.1 km. The AHe ages for the main transect range from 1.2 ± 0.2 Ma to 6.7 ± 0.3 Ma; ZHe ages for the main transect range from 7.7 ± 0.3 Ma to 14.1 ± 0.6 Ma (Fig. 4B; Tables 2 and 3). We include one additional AHe age in Figure 4B from a sample collected on the Yalong River 28 km north-northwest of the main transect at ~2500 m (wbo-04-19, Fig. 3B; * in Fig. 4B), but we did not include it in our analysis in order to focus our results and interpretation on the immediate vicinity of main Yalong (Li Qui) transect. The age (2.4 ± 0.3 Ma) is consistent with the main transect data. There is no break in slope exhibited in either the AHe or ZHe data.

Yangtze River

Our Yangtze transect was collected directly adjacent to the Yangtze River ~65 km south of the town of Batang in westernmost Sichuan (Fig. 3C). At the transect bottom, the Yangtze River is ~2300 m in

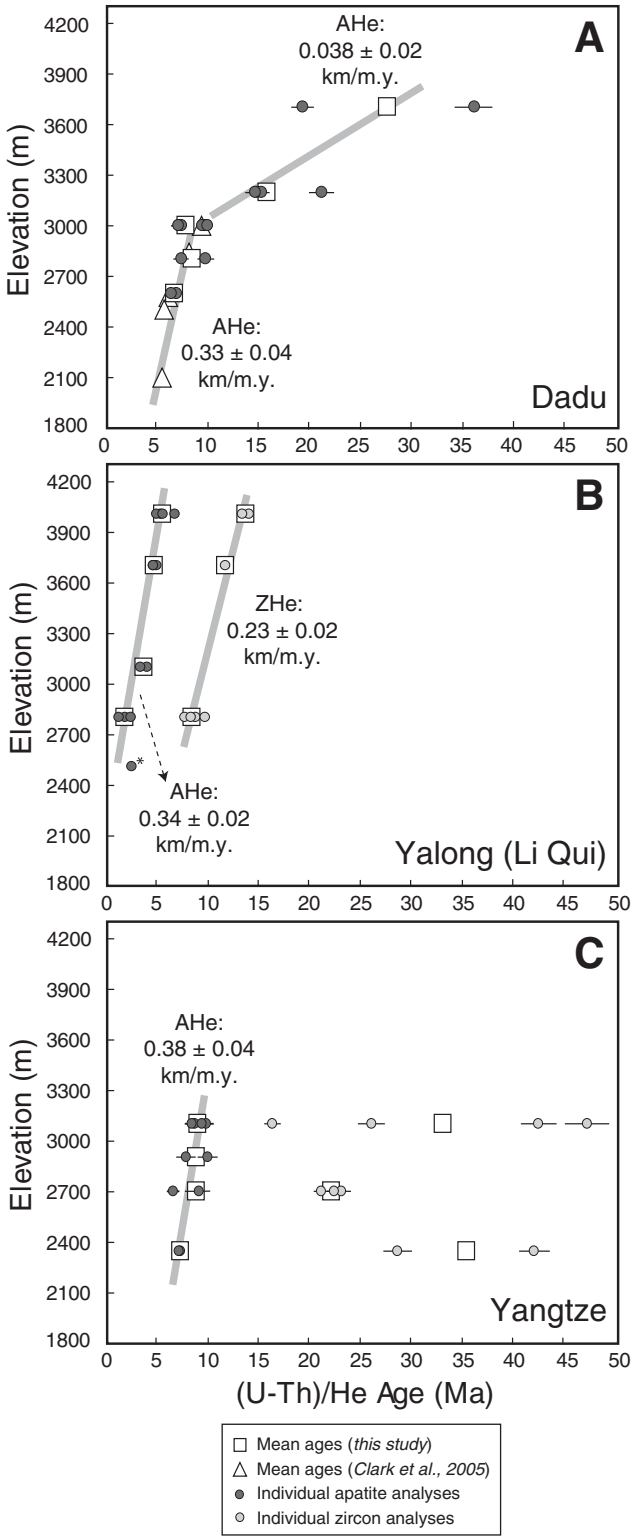

Figure 4. Transect data. Cooling age versus sample elevation for Dadu (A), Yalong (Li Qui) (B), and Yangtze (C) AHe and ZHe data. Individual cooling ages are plotted with 2σ analytical uncertainty. Bold gray lines indicate least-squares regression best-fit age-elevation gradients for individual ages for each transect; we do not fit the mean ages. The two fits for the Dadu transect are for all data ≥3000 m and all data ≤3000 m. Sample wbo-19–04, mentioned in the text in relation to the Yalong (Li Qui) transect, is noted with an asterisk.

elevation. Samples within the transect ranged in elevation from 2350 m to 3100 m and were collected over a horizontal distance of 5 km. The AHe ages for the transect range from 6.5 ± 0.3 Ma to 9.9 ± 0.4 Ma; ZHe ages for the transect range from 16.3 ± 0.8 Ma to 68.2 ± 3.0 Ma (Fig. 4C; Tables 2 and 3). The ZHe ages are scattered and generally have inconsistent replicate analyses (Fig. 4C); we therefore limit our discussion of the Yangtze ZHe ages. As with the Yalong transect, there is no break in slope exhibited in the AHe data.

EROSION AND INCISION RATES

The age-elevation relationships observed in our results allow us to estimate long-term rates of erosion and river incision on the eastern margin. All three transects indicate that AHe and ZHe ages are strongly correlated with elevation (Fig. 4). We used a least squares regression routine, which weights analytical uncertainty on the He ages as the dependent variable, to fit all age-elevation data (York, 1968). As noted already, on the Dadu (Jinchuan) transect, there is an inflection point in the age-elevation relationship at ~3000 m, implying a slow apparent erosion rate between 36.1 and ca. 10 Ma, followed by an acceleration in erosion from ca. 10 to 6.4 Ma. We therefore fit age-elevation data ≥3000 m and ≤3000 m. The fit for our data ≤3000 m predicts an apparent erosion rate of 0.33 ± 0.04 km/m.y. (or mm/yr); the fit for our data ≥3000 m predicts an apparent erosion rate of 0.038 ± 0.02 km/m.y. The inflection point in the age-elevation relationships therefore represents an ~10-fold increase in apparent erosion rate. A least squares regression fit to our data ≤3000 m combined with all of the Dadu (Danba) data from Clark et al. (2005) yields an apparent erosion rate of 0.27 ± 0.08 km/m.y., showing good agreement between the two data sets.

For the Yalong (Li Qui) transect, regression fits for apatite and zircon data predict an apparent erosion rate of 0.34 ± 0.02 km/m.y. for AHe and 0.23 ± 0.02 km/m.y. for ZHe. The linearity of both AHe and ZHe age-elevation plots implies steady erosion from 6.7 to 1.2 Ma and 14.1 to 7.7 Ma, respectively. There are no large inflection points in either AHe or ZHe data sets to suggest significant changes in apparent erosion rate. The relative consistency between AHe and ZHe erosion rates implies more or less steady erosion from ca. 14 Ma to 1.2 Ma, with a possible increase at ca. 7 Ma, though this apparent change may simply reflect the greater sensitivity of AHe transects to topographic deflection of isotherms (e.g., Reiners et al., 2003; Braun, 2005). Finally, for the Yangtze transect, regression fits for the AHe data predict an apparent erosion rate of 0.38 ± 0.04 km/m.y. The linearity of the AHe age-elevation plot implies a steady erosion rate from 9.9 to 6.5 Ma. As noted earlier, there is no inflection point in the AHe data to suggest a nonsteady erosion rate.

A composite plot of all mean AHe ages within the rapidly incising gorges (excluding the Dadu data >3000 m that reflect slower erosion prior to 10 Ma) displays regional agreement of age-elevation data (Fig. 5). All transects exhibit consistent apparent long-term erosion rates between 0.3 and 0.4 km/m.y. over the span of ages (ca. 10–6.5 Ma or ca. 10–2 Ma). We included in our composite analysis additional data from Clark et al. (2005). The Yalong (Juilong) transect data in Clark et al. (2005) were collected over a horizontal distance of ~50 km starting in Juilong and traveling south down to the Yalong River. These data sampling points were located ~70 km south-southeast from our Yalong (Li Qui) data. The elevation range of the Yalong (Juilong) data is 1700–2750 m; mean AHe ages range from ca. 4.6 to 10.1 Ma (Table 4; Fig. 5). The apparent erosion rate for the Yalong (Juilong) transect data is lower (0.22 ± 0.05 km/m.y.), but the error bars on these samples are high, and the ages and/or elevations are consistent with the Dadu and Yangtze data, and this transect is spread over an order of magnitude greater horizontal distance.

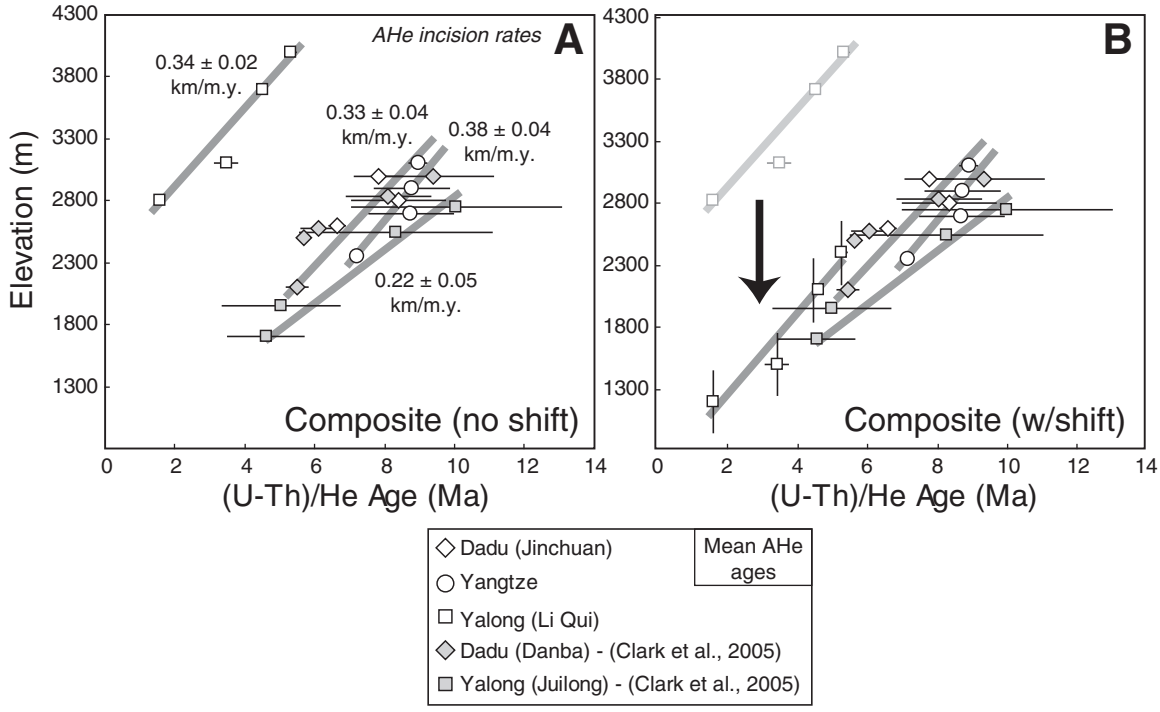

Figure 5. Composite plots of mean cooling age versus sample elevation for all transects. Mean cooling ages are plotted with 2σ error bars (representing the standard deviation from the spread of replicate values) (see Table 4). We include in these plots Dadu (Danba) and Yalong (Juilong) data from Clark et al. (2005). We exclude the upper part of the Dadu transect (i.e., data >3000 m) to focus on the post–10 Ma accelerated long-term erosion rates. (A) Composite plot for all data. (B) Composite plot for all data with a 1500–2000 m shift in the Yalong (Li Qui) data. We interpret the Li Qui study area to have experienced 1500–2000 m of young (post–ca. 2 Ma) uplift relative to other transects and associated rapid exhumation to offset the Li Qui data from Juilong ages collected ~70 km south-southeast, which match ages in the Dadu and Yangtze regions.

We used the zero-age concept to estimate erosion rates during the time interval between the youngest (lowest elevation) AHe age and the present (see Fig. 6 *in* Reiners and Brandon, 2006). Each age-elevation relationship predicts a zero AHe age (or *y*-intercept) that represents the present elevation of AHe closure if the erosion indicated by the data has not changed significantly from the youngest age to the present. The predicted modern closure elevations (i.e., intercepts) from our transect trends are ~400 m, ~2200 m, and ~100 m for the Dadu, Yalong (Li Qui), and Yangtze transects, respectively. If we assume a steady geothermal gradient of 30–40 °C/km during incision, a closure temperature of apatite of ~70 °C, and a surface temperature of 10 °C, the expected closure elevation for AHe is ~1.5–2 km beneath present mean elevations. For both the Dadu and Yangtze transects, the predicted modern closure elevations from the AHe age-elevation data are indeed ~1500–2000 m below present mean elevations using these assumptions, consistent with an approximately constant erosion rate (0.3–0.4 km/m.y.) from youngest AHe ages (ca. 5 Ma) to the present. For the Yalong (Li Qui) transect, however, there is only a ~200–400 m difference between the predicted modern AHe closure elevation and present mean elevation. We interpret this as evidence for an increase in apparent erosion rate from the youngest mean AHe age (ca. 2 Ma) to the present. The caveats to this analysis lie in the assumptions about the geothermal gradient and closure temperature, which may change underneath the valleys in response to incision. However, the discrepancy in the case of the Yalong (Li Qui) transect is too large to explain given realistic estimates of these parameters. We discuss this further in the following discussion.

The two different data sets (AHe and ZHe) for the Yalong (Li Qui) and Yangtze transects can be combined to analyze the interval of time between AHe and ZHe closure. For the Yalong (Li Qui) transect, this provides a check on the internal consistency of the erosion rates. There are three samples within the Yalong (Li Qui) transect with both AHe and ZHe ages; the difference between the two ages for these samples is 8.1–6.9 m.y. (average 7.3 m.y.). Assuming an AHe closure temperature of ~70 °C, a ZHe closure temperature of ~180 °C, and a geothermal gradient of 30–40 °C/km, the predicted distance between the closure AHe and ZHe is 2750 m. Combined with the difference between AHe and ZHe age, this yields an erosion rate between 0.33 and 0.39 km/m.y., consistent with the apparent erosion rates from the age-elevation fits. We interpret this as evidence supporting a steady long-term erosion rate for the Yalong (Li Qui) area from ca. 14 Ma to 1.2 Ma. The scattered ZHe data in the Yangtze transect, meanwhile, do not allow for detailed analysis, but one sample within the Yangtze transect did yield consistent ZHe replicate ages. The difference between AHe and ZHe ages for this sample is 14.4 m.y. (Fig. 4C). Using similar parameters as the previous calculation, this yields an erosion rate of ~0.19 km/m.y. between ca. 23 Ma (ZHe closure) and 9 Ma (AHe closure) for this transect. This implies that there was an increase in apparent erosion rate between 23 and 10 Ma for the Yangtze transect area, since the AHe age-elevation data indicate that the apparent erosion rate from 9.9 to 6.5 Ma was 0.38 ± 0.04 km/m.y.

ONSET OF RAPID EXHUMATION AND RIVER INCISION

Our data provide valuable constraints on the timing of rapid river incision within the Dadu, Yalong, and Yangtze River gorges on the eastern margin of the Tibetan Plateau. Clark et al. (2005) argued for regional

accelerated erosion in the Dadu and Yalong River gorges into slowly eroding, relict topography on the eastern margin beginning between 9 to 13 Ma, but they could not confirm the acceleration in a single age-elevation transect. Our new AHe data in the Dadu River gorge near Jinchuan indicate that rapid incision of ~0.33 mm/yr began at ca. 10 Ma and has not changed significantly since that time. The piecewise linear regressions in Figure 4A indicate that rapid incision began quickly and was well established by ca. 10 Ma. A more conservative interpretation of the data would say that rapid incision occurred after 11–12 Ma and was well established by ca. 9 Ma. The AHe and ZHe data in the Yangtze River gorge near Batang similarly indicate that rapid incision of ~0.38 mm/yr began after 22 Ma and prior to 10 Ma, and has continued to the present. We discuss additional constraints on the timing of rapid river incision for the Yangtze later herein. The AHe and ZHe data in the Yalong River gorge adjacent to the lower Li Qui River, meanwhile, indicate that rapid incision of ~0.34 mm/yr began prior to 14 Ma, or that it was at least well established by ca. 12–14 Ma. Rapid incision associated with the Yalong (Li Qui) transect continued into the early Quaternary, but it has since increased. This transect is distinct from regionally consistent incision histories elsewhere.

The general agreement among elevations, ages, and apparent erosion displayed in Figure 5 for each of the Dadu, Yangtze, and Yalong (Juilong) transects reflects the fact that these transects come from positions on the trunk rivers with comparable elevations and relief (i.e., incision below relict topography) (Fig. 1). At the time of AHe closure for these transects, the closure isotherm had to be at about the same elevation for the ages and elevations to agree (given the same erosion rate and similar geothermal gradients). Assuming the mapped remnants of relict topography adjacent to the Dadu and Yangtze transects are correct (i.e., Clark et al., 2006), the similar elevations, ages, and apparent erosion rates for these transects imply similar timing for rapid incision into relict topography. The timing of rapid incision is well constrained for the Dadu at ca. 10 Ma, and, where it was observed in the transect (i.e., at ~3000 m elevation), it is consistent with estimated elevations of relict topography in surrounding areas (4200–4500 m). This would suggest, then, that the Yangtze River gorge started incising rapidly at ca. 10 Ma as well, and that our highest elevation sample in the Yangtze transect (3100 m) was close to the inflection point given that it rests ~1500 m below surrounding remnants of relict topography. Moreover, the total incision depth below the relict surface for the Yangtze transect region (~2.5 km; see Fig. 1) is consistent with a conservative range of steady incision rates between 0.25 and 0.4 km/m.y. over the past 6–10 m.y., but no longer. Thus, although our thermochronometric data may allow an earlier initiation of rapid exhumation, our data combined with geomorphic evidence for preserved relict topography above the Yangtze transect argue against it.

In the case that the mapped remnants of relict topography adjacent to the Yangtze transect are incorrect, we have limited constraints on the initiation of incision. Our interpretation of the scatter observed in the Yangtze ZHe data is that it provides evidence that the column of rock represented in this transect eroded slowly through the partial retention zone (PRZ) of ZHe, implying that the duration of rapid incision (0.38 ± 0.04 km/m.y.) has not been long enough to expose ZHe ages representing this younger phase. This would suggest that there has been less than ~4.3–5.7 km of total exhumation here, implying an onset of 0.38 km/m.y. incision no earlier than 11–15 Ma. This is supported by the time interval between the AHe and ZHe ages, which suggests that there was an increase in erosion rate between 23 and 10 Ma.

Our ability to constrain the onset of river incision near our Yangtze River data rests, therefore, on the interpretation of the mapped remnants presented in Clark et al. (2006). Numerous remnants of relict topography have been mapped near our Yangtze data, but the extent of surface dissection by tributaries and modification by glacial erosion varies. One particular remnant of relict topography discussed by Clark et al. (2006) is the "Daocheng" surface. It is located halfway between the Yalong and Yangtze Rivers west of our Yangtze transect data (see Figs. 9d and 9e *in* Clark et al., 2006), displays characteristic relict topography morphology, and has uniformly old AHe ages (Clark et al., 2005). Clark et al. (2006) interpreted this surface to extend, interrupted by a few incised tributaries, over to the location of our Yangtze transect, and hypothesized it to connect to the smaller patches of relict topography mapped near our Yangtze River data. We accept this argument here, adding the caveat that because the mapped remnants near our Yangtze data display minor to moderate surface modification by tributary dissection and glacial erosion (as observed in an analysis of satellite imagery and topographic data), there is greater certainty in the estimated elevation of pre-incision topography. Given this caveat and the various constraints discussed already, our favored interpretation is that rapid incision for the Yangtze River gorge began between 10 and 15 Ma.

There are no well-preserved remnants of relict topography directly near the Yalong (Juilong) transect of Clark et al. (2005) to allow for a similar estimate of the timing of rapid incision. Assuming that the area around the Yalong (Juilong) transect did experience accelerated erosion into prior, relict topography, the lack of well-preserved remnants suggests that either rapid incision did initiate ca. 10 Ma, but erosion has been significant enough to inhibit identification of remnants, or that rapid incision began prior to ca. 10 Ma and the relict topography was originally at a higher elevation in this region.

DISCUSSION

Yalong (Li Qui) Transect: Earlier Onset of Rapid Incision and Quaternary Increase

Our Yalong (Li Qui) transect exhibits the same erosion rate as the other transects, but it exposes younger AHe ages (Fig. 5). As discussed earlier, these younger AHe ages result in a ~1500 m discrepancy between the predicted and expected AHe closure elevations, requiring an increase in apparent erosion rate after 1.2 Ma. The Yalong (Li Qui) transect is also shifted ~1500 m from all other data (Fig. 5B). The age-elevation relationship exhibited by the Yalong (Li Qui) transect matches the expected age-elevation relationship for samples at depth beneath the Dadu and Yangtze transect, between the bottom elevation of each transect and the closure depth. This suggests that between at least ca. 10 and 1.2 Ma, the Yalong (Li Qui), Dadu, and Yangtze transects were all eroding at the same erosion rate, and each closure isotherm for AHe was at a similar elevation, implying a broad, synchronous pattern of river incision into an uplifted (or uplifting) plateau as interpreted by Clark et al. (2006). Then, after 1.2 Ma, the Yalong (Li Qui) experienced additional uplift and enhanced exhumation to offset and expose the column of rock preserving the 10–1.2 Ma cooling ages. Both the discrepancy between the predicted and observed closure depth of apatites for this transect and this offset with the other transects suggest that the additional uplift and exhumation in the area of the Yalong (Li Qui) transect are on the order of ~1500 m, implying an erosion rate of 1–1.5 mm/yr since the middle Quaternary.

The Yalong (Li Qui) transect therefore has two interesting aspects that deviate from the Dadu and Yangtze transects: (1) rapid incision started earlier in this region, prior to ca. 14 Ma; and (2) it has recently been influenced by additional uplift and exhumation. The earlier initiation indicates that this area had already exhumed at least 1400 m before 10 Ma. This minimum estimate and the additional Quaternary component imply a minimum of 3000 m more total exhumation in the area of the Yalong

(Li Qui) transect than in the other gorges. This is supported by the topography of the area around the Yalong (Li Qui) transect (Fig. 6). There are no remnants of relict topography preserved, mean elevations are higher, and there is evidence of a higher degree of glacial erosion (i.e., depth of alpine glacier valleys, cirque wall heights, number and size of glacial lakes, run-out of moraines, etc.) than that seen in topography to the north or south. Assuming that relict topography once existed around the Yalong (Li Qui) transect, this implies that this area has experienced more rock uplift and that rivers (and glaciers) have eroded more material.

What accounts for these deviations of the Yalong (Li Qui) transect? What is responsible for the uplift and additional increase in the Quaternary? Why did rapid incision start earlier but with the same rate of incision as the other gorges? The Quaternary uplift and exhumation of the Yalong (Li Qui) transect are possibly related to young, active, and rapid deformation associated with the Gongga Shan area. Topography near Gongga Shan rises above the relict landscape and exhibits numerous signs of rapid (>1 mm/yr) uplift, erosion, and river incision (Clark et al., 2005; Ouimet et al., 2009). Very young AHe ages have also been observed near Gongga Shan (Clark, 2003; location indicated in Fig. 2; mean age is given in Table 4). Another aspect of tectonics to consider in this region is that uplift and exhumation may be associated with a young, active fault. The major active faults in the area are the left-lateral Xianshuihe and Litang faults (Fig. 2). One structure in particular between these two faults runs southwest-northeast, separating our Yalong (Li Qui) and Yalong (Juilong) transect data, and it might account for the offset data between the AHe data sets (fault A on Figs. 2 and 6). This fault has been mapped with both strike-slip and thrust motion (Burchfiel et al., 1995), and it could be accommodating local transpressional deformation in between the larger active faults, accounting for the Quaternary deformation, uplift, and exhumation. Differential isostatic response to river incision and glacial erosion of high topography may have contributed to amplify this localized tectonic uplift (e.g., Zeitler et al., 2001). A similar argument for local uplift associated with smaller faults and deformation in between larger, more active systems and enhancement due to erosional unloading has been proposed for the Snow Mountains area of the Yangtze River (location: 27.2388°N, 100.1376°E) (Studnicki-Gizbert et al., 2005). Both can be viewed as local structural perturbations superimposed on the broad regional pattern of uplift and river incision documented by Clark et al. (2006).

A Pliocene-Pleistocene (ca. 2 Ma) pulse of accelerated incision within the Himalayan-Tibetan orogenic system has also been recognized along the Himalayan range front (Huntington et al., 2006), where thermochronologic data show a fivefold increase in erosion rate between 2.5 and 0.9 Ma. In the absence of a clear tectonic explanation for enhanced erosion, Huntington et al. (2006) argued for Pliocene-Pleistocene climate change being responsible for the increase (i.e., the onset of Northern Hemisphere glaciation and an intensification of the Asian monsoon). Though our results suggest similar timing and magnitude of accelerated erosion after 2 Ma, the relatively localized nature of the deviation observed in our Yalong (Li Qui) transect, particularly in comparison with the other transects presented in this paper, seems to support the local tectonics and/or fault-related explanations discussed here rather than a regional climate change.

The earlier onset of rapid incision in the Yalong (Li Qui) area compared to the Dadu area is harder to conclusively explain. One explanation for the earlier onset of rapid incision is that the Yalong (Li Qui) transect may have experienced local uplift and exhumation associated with deformation along the Yalong thrust belt prior to regional, long-wavelength uplift and subsequent incision of major rivers (Fig. 2). A second explanation is that it might be related to the transient nature of large river response and incision

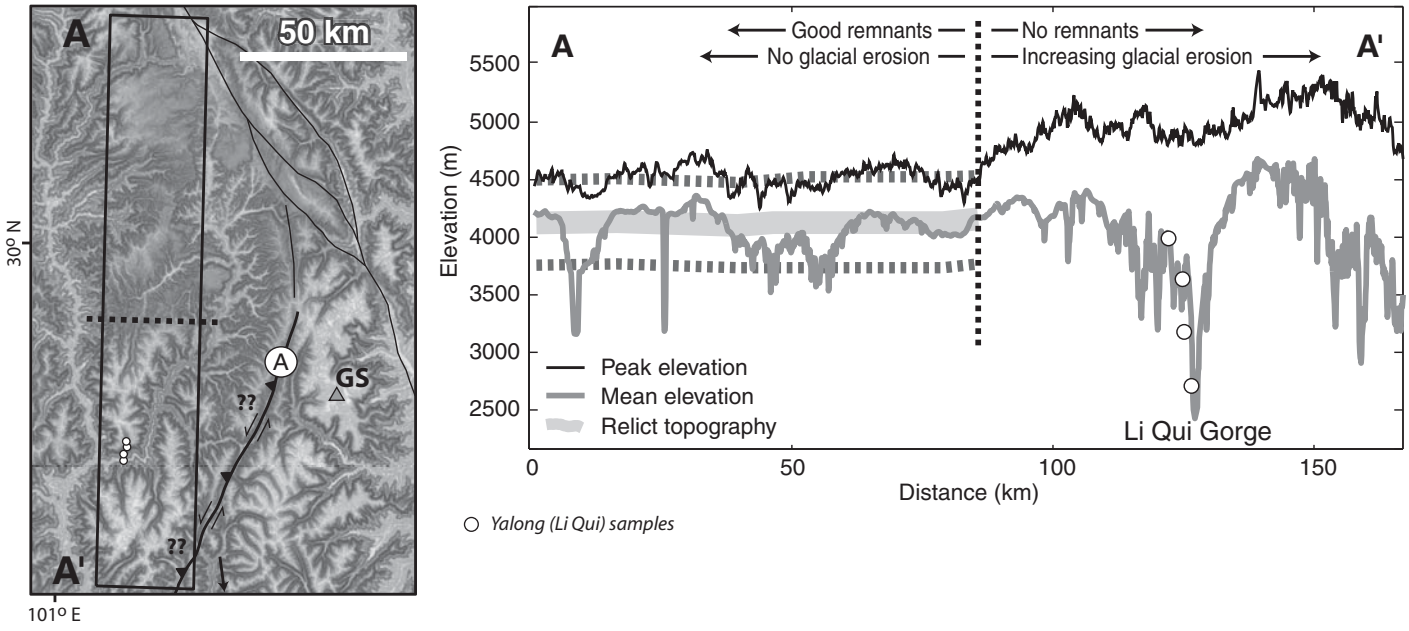

Figure 6. Topographic swath profile near the Yalong (Li Qui) transect. The topography around the Yalong (Li Qui) transect is higher, has no remnants of relict topography preserved, and displays evidence of a higher degree of glacial erosion than topography to the north. Assuming that relict topography once existed around the Yalong (Li Qui) transect, this implies that this area has experienced more surface uplift and that rivers (and glaciers) have eroded more material. Location "A" marks the fault discussed in the text, also indicated in Figure 2. Bold light-gray line indicates well-preserved remnants of relict topography, with the typical ±500 m relief for relict topography indicated by dashed gray lines (see Clark et al., 2006). The Yalong (Juilong) data discussed in the text are located ~100 km S of the arrow at the bottom of the map. The location of Yalong (Li Qui) transect samples shown in the topographic profile are approximate; this is due to the fact that they are drawn on the mean topography line. GS—Gongga Shan.

following uplift. First, exhumational response may have been faster where local deformation produced greater relief (e.g., in the Longmen Shan and along the Yalong thrust belt) with a greater lag time experienced by rivers subjected only to long-wavelength uplift. Second, incision may have initiated later at the Dadu transect simply because it is both a smaller river, and, prior to a hypothesized recent capture event, the transect may have been farther upstream in the regional river network. Clark et al. (2004) documented evidence that the Dadu River was originally a tributary to the Yalong, entering the Yalong just upstream of its confluence with the Yangtze, placing the Dadu transect considerably farther upstream. Regardless of the exact cause of the earlier onset for the Yalong (Li Qui) transect in particular, an intriguing outstanding question is: why is the rate of exhumation so regionally consistent despite differences in the timing of the onset of rapid exhumation and apparent driving mechanisms (i.e., local uplift on upper-crust structures versus regional uplift and/or incision into a previously uplifted plateau following a regional climate change)?

Regional Incision of the Eastern Margin of the Tibetan Plateau

We interpret our AHe and ZHe results and the topographic context of each transect to show onset of accelerated incision at ca. 10 Ma for the Dadu, 10–15 Ma for the Yangtze, and >14 Ma for the Yalong (Li Qui) transect. Despite the earlier onset of rapid exhumation at the position of the Yalong transect, exhumation (river incision) rates are remarkably consistent during the ca.10–2 Ma interval. We argue that these results support the notion that incision of major rivers across the entire eastern margin was relatively synchronous. Although an upstream-propagating wave of incision is expected (e.g., Whipple and Tucker, 1999), river incision models predict steady vertical propagation rates (Niemann et al., 2001; Wobus et al., 2006), and thus the similar elevations of our transects imply similar arrival times despite different distances upstream in the network. Broad long-wavelength uplift of the plateau documented in the distribution of low-relief topographic remnants (Clark et al., 2006) had to be contemporaneous with, or precede, canyon incision. Relatively uniform amounts of total uplift across the study area (Clark et al., 2006; Fig. 1) and synchronous river incision imply spatially uniform uplift over much of the region. The similar timing of the onset of rapid exhumation in much of the Longmen Shan at 8–12 Ma (Kirby et al., 2002; Kirby, 2008; Godard et al., 2009), where plateau uplift has created a topographic front that rivals the Himalaya, supports the interpretation of previous researchers that any lag time between uplift and exhumation was probably short.

The different history recorded in the Yalong (Li Qui) transect appears to reflect both early deformation along the Yalong thrust belt (see discussion in Clark et al., 2006) and Quaternary deformation on local structures. This interpretation is supported by geomorphic evidence, including local topography that exceeds the elevation of the regional surface reconstructed by Clark et al. (2006), and the erosional removal of the low-relief surface. Localized uplift and exhumation appear to be superimposed on the broad regional uplift discussed already.

Although we favor the interpretation of the onset of accelerated incision as reflecting the regional response of major rivers to regional uplift, it is important to note that there may have been a delay time (possibly millions of years) between the pulse of rock uplift regionally and the incisional response of major rivers hundreds of kilometers upstream from the plateau edge. With that caveat, our constraints on the onset of accelerated river incision into the high topography throughout the eastern margin can be used as a proxy for regional plateau uplift. It is widely believed that uplifting topography of the Himalayan-Tibetan orogenic system induced climatic changes, such as strengthened precipitation related to broad climate changes and local elevation effects (orography) (Ruddiman and Kutzbach, 1989; Prell and Kutzbach, 1997; An et al., 2001). In this context, it is likely that the combination of uplifting topography (resulting in relative base-level lowering of major rivers in the region) and increased precipitation acted together to increase stream power and begin incision into plateau. This link between uplifting topography and strengthened precipitation suggests that incision was coeval with uplift rather than significantly lagging behind. Furthermore, while we acknowledge that low gravel fluxes off the low-relief relict landscape may have slowed river incision (e.g., Pelletier, 2007), it is unlikely that paleoclimatic conditions were sufficiently arid in the region prior to ca. 10 Ma to have greatly delayed river incision following regional uplift.

In addition to regional uplift initiating incision, the topographic evolution of the eastern margin may also have included stream capture events (likely induced after regional uplift and incision had began; e.g., Clark et al., 2004) and differential isostatic adjustment to regional erosion. We see these aspects as secondary controls on uplift and incision that are likely to have occurred after regional uplift and incision had already begun. They may help to generally explain the overall variation in the onset of rapid incision in the Dadu (ca. 10 Ma), Yangtze (10–15 Ma), and Yalong (>14 Ma). However, the regional consistency of the helium ages, elevations, and incision rates seems to suggest that if these secondary aspects have modified things, their magnitude is not great. Some of the variability presently observed in the high-elevation topography in general (i.e., well-preserved remnants of relict topography versus topography that looks much more glacially modified) might well be the result of variations in relief at the time uplift began. As higher elevations were attained regionally, these locally high areas would have experienced more intense glacial erosion and could have induced local isostatic compensation. In this case, we do not expect the magnitude of isostatic compensation to have affected the regional picture, but it is important to consider such effects since they may be responsible for the modification of the uplifted relict landscape, which is an important feature used to constrain regional uplift and incision to begin with. We would also expect that the cutting of the river gorges would initiate an isostatic response of mean topography, but again we do not see this as exerting a major control on the rates and timing of accelerated incision. The degree to which these secondary aspects might affect the rates and timing of accelerated incision requires further examination beyond the scope of this paper.

The estimates of apparent long-term erosion rates are not particularly high, especially when compared to long-term erosion rates observed in the Himalaya (1–10 km/m.y.; e.g., Zeitler, 1985; Burbank et al., 2003; Huntington et al., 2006). Though not the magnitude of Himalayan erosion, these long-term rates are consistent with short-term (10^2–10^5 yr) erosion rates measured with cosmogenic nuclides for the deeply incised river gorges (Ouimet et al., 2009). In fact, the estimates of the long-term erosion both before and after the initiation of rapid incision are consistent with the observed distribution of short-term erosion rates. Short-term erosion rates range from ~0.030 to 3 km/m.y., generally reflecting either slow erosion associated with low-relief, relict topography (<0.05 km/m.y.), or fast erosion associated with incised river gorges (>0.4 km/m.y.) (Ouimet et al., 2009; Harkins et al., 2007). The slow, pre–rapid incision, long-term rate is constrained in only one location (Dadu transect, 0.038 ± 0.02 km/m.y.), but it agrees with both the slow cooling recorded in the Longmen Shan before the onset of rapid exhumation (Kirby et al., 2002; Godard et al., 2009) and short-term rates representative of the same type of topography (Ouimet et al., 2009). The general discrepancy between upland short-term and long-term erosion rates recorded in canyons supports the idea that this landscape is still

actively involved in a large-scale transient response to regional uplift, exhibiting disequilibrium rates of erosion and river incision as a function of location within these large river systems.

One final interesting aspect to our results is that the onset of acceleration incision at ca. 10 Ma in the Dadu River matches accelerated incision recognized along the Himalayan range front (Wobus et al., 2008). Furthermore, Wobus et al. (2008) documented erosion rates <0.1 km/m.y. prior to 10 Ma and ~0.5 km/m.y. after 10 Ma, i.e., very similar to our Dadu results. This suggests a connection between margins of the Himalayan-Tibetan orogenic system. Our result for the Dadu River, in particular, is in fact broadly consistent with shifts in both climate and tectonics observed on all of the margins of the Himalayan-Tibetan orogenic system in the late Miocene (8–10 Ma) based on various lines of evidence (see Molnar, 2005, and references therein). However, the Yalong transect records an earlier onset of rapid exhumation, and records remain rather sparse across a wide expanse of the eastern margin of the Tibetan Plateau. Additional research may well reveal additional complexity in the timing of deformation and exhumation, particularly along the structurally controlled margins of the plateau.

CONCLUSIONS

Our data set provides new, important constraints on the rates of exhumation in major rivers on the eastern margin of the Tibetan Plateau and the timing of rapid incision. We have both confirmed and more tightly constrained the previously hypothesized notion of broad, plateau uplift and subsequent incision by major rivers (Clark et al., 2005). Our data suggest that a broad area within the eastern margin of the Tibetan Plateau, encompassing the Dadu River adjacent to the Sichuan Basin and Yangtze River ~450 km to the west, was being incised by 10 Ma and that incision into high topography has been relatively constant and uniform in the region throughout the late Cenozoic (with rates between 0.3 and 0.4 km/m.y.). These results provide valuable constraints for geodynamic models exploring the late Cenozoic evolution of this part of the Tibetan Plateau (e.g., ways in which topography grew and uplift progressed). Furthermore, we quantify the details of exhumation, the specifics of timing, and the effects of local tectonics, paleotopography, and dynamics of large-scale river adjustment. The AHe and ZHe data in the Yalong River gorge reveal a more dynamic cooling and exhumation history, with >3000 m more exhumation than other river gorges. Data indicate that rapid incision began prior to ca. 14 Ma, continued to the early Quaternary, and then increased again, likely in response to local uplift and erosion associated with active faults in the region. The earlier onset of rapid incision in the Yalong River gorge compared to the Dadu suggests local deviation from the simple regional context of long-wavelength uplift on the eastern margin and subsequent incision by major rivers.

ACKNOWLEDGMENTS

This work was funded by National Science Foundation (NSF) Continental Dynamics program (EAR-0003571) and completed in collaboration with Clark Burchfiel at Massachusetts Institute of Technology and Zhiliang Chen and Tang Fawei at the Chengdu Institute of Geology and Mineral Resources (Sichuan, China). Special thanks are due to Jamon Frostenson, Joel Johnson, and Miu Guoxia for assistance in the field, Stefan Nicolescu for expert help with (U-Th)/He analyses, and Donelick Analytic for apatite and zircon separation. We also wish to thank Taylor Schildgen, Kristen Cook, and Scott Miller for helpful feedback and discussion, as well as Bodo Bookhagen, Brian Horton, and Jon Pelletier for their reviews.

REFERENCES CITED

An, Z., Kutzbach, J.E., Prell, W.L., and Porter, S.C., 2001, Evolution of the Asian monsoons and phased uplift of the Himalayan-Tibetan Plateau since late Miocene times: Nature, v. 411, p. 62–66, doi: 10.1038/35075035.

Arne, D., Worley, B., Wilson, C., Chen, S.F., Foster, D., Luo, Z.L., Liu, S.G., and Dirks, P., 1997, Differential exhumation in response to episodic thrusting along the eastern margin of the Tibetan Plateau: Tectonophysics, v. 280, p. 239–256, doi: 10.1016/S0040-1951(97)00040-1.

Braun, J., 2005, Quantitative constraints on the rate of landform evolution derived from low-temperature thermochronology: Reviews in Mineralogy and Geochemistry, v. 58, p. 351–374, doi: 10.2138/rmg.2005.58.13.

Burbank, D.W., Blythe, A.E., Putkonen, J., Pratt-Sitaula, B., Gabet, E., Oskin, M., Barros, A., and Ojha, T.P., 2003, Decoupling of erosion and precipitation in the Himalayas: Nature, v. 426, p. 652–655, doi: 10.1038/nature02187.

Burchfiel, B.C., Chen, Z., Liu, Y., and Royden, L.H., 1995, Tectonics of the Longmen Shan and adjacent regions, central China: International Geology Review, v. 37, p. 661–735, doi: 10.1080/00206819509465424.

Chen, S.F., and Wilson, C.J.L., 1996, Emplacement of the Longmen Shan thrust-nappe belt along the eastern margin of the Tibetan Plateau: Journal of Structural Geology, v. 18, p. 413–430, doi: 10.1016/0191-8141(95)00096-V.

Chen, S.F., Wilson, C.J.L., and Worley, B.A., 1995, Tectonic transition from the Songpan-Garze fold belt to the Sichuan Basin, southwestern China: Basin Research, v. 7, p. 235–253, doi: 10.1111/j.1365-2117.1995.tb00108.x.

Clark, M.K., 2003, Late Cenozoic uplift of southeastern Tibet [Ph.D. thesis]: Cambridge, Massachusetts, Massachusetts Institute of Technology, 226 p.

Clark, M.K., Schoenbohm, L.M., Royden, L.H., Whipple, K.X., Burchfiel, B.C., Zhang, X., Tang, W., Wang, E., and Chen, L., 2004, Surface uplift, tectonics, and erosion of eastern Tibet from large-scale drainage patterns: Tectonics, v. 23, TC1006, doi: 10.1029/2002TC001402.

Clark, M.K., House, M.A., Royden, L.H., Whipple, K.X., Burchfiel, B.C., Zhang, X., and Tang, W., 2005, Late Cenozoic uplift of southeastern Tibet: Geology, v. 33, p. 525–528, doi: 10.1130/G21265.1.

Clark, M.K., Royden, L.H., Whipple, K.X., Burchfiel, B.C., Zhang, X., and Tang, W., 2006, Use of a regional, relict landscape to measure vertical deformation of the eastern Tibetan Plateau: Journal of Geophysical Research, v. 111, F03002, doi: 10.1029/2005JF000294.

Dirks, P.H.G.M., Wilson, C.J.L., Chen, S., Luo, Z.L., and Liu, S., 1994, Tectonic evolution of the NE margin of the Tibetan Plateau; evidence from the central Longmen Mountains, Sichuan Province, China: Journal of Southeast Asian Earth Sciences, v. 9, p. 181–192, doi: 10.1016/0743-9547(94)90074-4.

Ehlers, T.A., 2005, Crustal thermal processes and the interpretation of thermochronometer data: Reviews in Mineralogy and Geochemistry, v. 58, p. 315–350, doi: 10.2138/rmg.2005.58.12.

Farley, K.A., 2000, Helium diffusion from apatite: General behavior as illustrated by Durango fluorapatite: Journal of Geophysical Research–Solid Earth, v. 105, p. 2903–2914, doi: 10.1029/1999JB900348.

Godard, V., Pik, R., Lavé, J., Cattin, R., Tibari, B., de Sigoyer, J., Pubellier, M., and Zhu, J., 2009, Late Cenozoic evolution of the central Longmen Shan, eastern Tibet: Insight from (U-Th)/He thermochronometry: Tectonics, v. 28, TC5009, doi: 10.1029/2008TC002407.

Harkins, N.W., Kirby, E., Heimsath, A.M., Robinson, R., and Reiser, U., 2007, Transient fluvial incision in the headwaters of the Yellow River, northeastern Tibet, China: Journal of Geophysical Research, v. 112, F03S04, doi: 10.1029/2006JF000570.

Huntington, K.W., Blythe, A., and Hodges, K., 2006, Climate change and late Pliocene acceleration of erosion in the Himalaya: Earth and Planetary Science Letters, v. 252, p. 107–118, doi: 10.1016/j.epsl.2006.09.031.

Kirby, E., 2008, Geomorphic insights into the growth of eastern Tibet and implications for the recurrence of great earthquakes: Eos (Transactions, American Geophysical Union), v. 89, no. 53, fall meeting supplement, abs. T24B-03.

Kirby, E., Reiners, P.W., Krol, M.A., Whipple, K.X., Hodges, K.V., Farley, K.A., Tang, W., and Chen, Z., 2002, Late Cenozoic evolution of the eastern margin of the Tibetan Plateau: Inferences from $^{40}Ar/^{39}Ar$ and (U-Th)/He thermochronology: Tectonics, v. 21, no. 1, 1001, doi: 10.1029/2000TC001246.

Mancktelow, N.S., and Grasemann, B., 1997, Time-dependent effects of heat advection and topography on cooling histories during erosion: Tectonophysics, v. 270, p. 167–195, doi: 10.1016/S0040-1951(96)00279-X.

Molnar, P., 2005, Mio-Pliocene growth of the Tibetan Plateau and evolution of East Asian climate: Palaeontologia Electronica, v. 8, no. 1, p. 1–23.

Niemann, J.D., Gasparini, N.M., Tucker, G.E., and Bras, R.L., 2001, A quantitative evaluation of Playfair's law and its use in testing long-term stream erosion models: Earth Surface Processes and Landforms, v. 26, p. 1317–1332, doi: 10.1002/esp.272.

Niemi, N., Clark, M., House, M., Royden, L., and Zhang, X., 2003, Late Cenozoic extension and exhumation of mid-crustal rocks at Gonga Shan, eastern Tibet: Geophysical Research Abstracts, v. 5, p. 12918.

Ouimet, W.B., 2007, Dissecting the eastern margin of the Tibetan Plateau: A study of landslides, erosion and river incision in a transient landscape [Ph.D. thesis]: Cambridge, Massachusetts, Massachusetts Institute of Technology, 197 p.

Ouimet, W.B., Whipple, K.X., and Granger, D.E., 2009, Beyond threshold hillslopes: Channel adjustment to base-level fall in tectonically active mountain ranges: Geology, v. 37, p. 579–582, doi: 10.1130/G30013A.1.

Pelletier, J.D., 2007, Numerical modeling of the Cenozoic fluvial evolution of the southern Sierra Nevada, California: Earth and Planetary Science Letters, v. 259, p. 85–96, doi: 10.1016/j.epsl.2007.04.030.

Prell, W.L., and Kutzbach, J.E., 1997, The impact of Tibet-Himalayan elevation on the sensitivity of the monsoon climate system to changes in solar radiation, *in* Ruddiman, W., ed., Tectonic Uplift and Climate Change: New York, Plenum Press, p. 171–201.

Qingzhou, L., Lin, D., Hongwei, W., Yahui, Y., and Fulong, C., 2007, Constraining the stepwise migration of the eastern Tibetan Plateau margin by apatite fission track thermochronology: Science in China Series D, Earth Science, v. 50, no. 2, p. 172–183.

Reid, A.J., Wilson, C.J.L., Phillips, D., and Liu, S., 2005, Mesozoic cooling across the Yidun Arc, central-eastern Tibetan Plateau: A reconnaissance Ar-40/Ar-39 study: Tectonophysics, v. 398, p. 45–66, doi: 10.1016/j.tecto.2005.01.002.

Reiners, P.W., 2003, (U-Th)/He dating and calibration of low-T thermochronometry: Geochimica et Cosmochimica Acta, v. 67, p. A395.

Reiners, P.W., 2005, Zircon (U-Th)/He thermochronometry: Reviews in Mineralogy and Geochemistry, v. 58, p. 151–179, doi: 10.2138/rmg.2005.58.6.

Reiners, P.W., and Brandon, M.T., 2006, Using thermochronology to understand orogenic erosion: Annual Review of Earth and Planetary Sciences, v. 34, p. 419–466, doi: 10.1146/annurev.earth.34.031405.125202.

Reiners, P.W., Zhou, Z.Y., Ehlers, T.A., Xu, C.H., Brandon, M.T., Donelick, R.A., and Nicolescu, S., 2003, Post-orogenic evolution of the Dabie Shan, eastern China, from (U-Th)/He and fission-track thermochronology: American Journal of Science, v. 303, p. 489–518, doi: 10.2475/ajs.303.6.489.

Reiners, P.W., Spell, T.L., Nicolescu, S., and Zanetti, K.A., 2004, Zircon (U-Th)/He thermochronometry: He diffusion and comparisons with Ar-40/Ar-39 dating: Geochimica et Cosmochimica Acta, v. 68, p. 1857–1887, doi: 10.1016/j.gca.2003.10.021.

Roger, F., Calassou, S., Lancelot, J., Malavieille, J., Mattauer, M., Xu, Z.Q., Hao, Z.W., and Hou, L.W., 1995, Miocene emplacement and deformation of the Konga-Shan Granite (Xianshui-He fault zone, West Sichuan, China): Geodynamic implications: Earth and Planetary Science Letters, v. 130, p. 201–216, doi: 10.1016/0012-821X(94)00252-T.

Roger, F., Malavieille, J., Leloup, P.H., Calassou, S., and Xu, Z., 2004, Timing of granite emplacement and cooling in the Songpan-Garze fold belt (eastern Tibetan Plateau) with tectonic implications: Journal of Asian Earth Sciences, v. 22, p. 465–481, doi: 10.1016/S1367-9120(03)00089-0.

Ruddiman, W.F., and Kutzbach, J.E., 1989, Forcing of late Cenozoic Northern Hemisphere climate by plateau uplift in southern Asia and the American West: Journal of Geophysical Research, v. 94, p. 18,409–18,427, doi: 10.1029/JD094iD15p18409.

Schoenbohm, L., Whipple, K., and Burchfiel, B.C., 2004, River incision into a relict landscape along the Ailao Shan shear zone and Red River fault in Yunnan Province, China: Geological Society of America Bulletin, v. 116, p. 895–909, doi: 10.1130/B25364.1.

Studnicki-Gizbert, C., Wang, Y., Burchfiel, B.C., and Chen, L., 2005, The Yulong mountains structural culmination: Tectonic and geomorphic controls on localized uplift rates and exhumation: Eos (Transactions, American Geophysical Union), v. 86, no. 52, fall meeting supplement, abs. T24C-07.

Stuwe, K., White, L., and Brown, R., 1994, The influence of eroding topography on steady-state isotherms—Application to fission-track analysis: Earth and Planetary Science Letters, v. 124, p. 63–74, doi: 10.1016/0012-821X(94)00068-9.

Wagner, G.A., and Reimer, G.M., 1972, Fission track tectonics: The tectonic interpretation of fission track ages: Earth and Planetary Science Letters, v. 14, p. 263–268, doi: 10.1016/0012-821X(72)90018-0.

Wallis, S., Tsujimori, T., Aoya, M., Kawakami, T., Terada, K., Suzuki, K., and Hyodo, H., 2003, Cenozoic and Mesozoic metamorphism in the Longmenshan orogen: Implications for geodynamic models of eastern Tibet: Geology, v. 31, p. 745–748, doi: 10.1130/G19562.1.

Whipple, K.X., 2004, Bedrock rivers and the geomorphology of active orogens: Annual Review of Earth and Planetary Sciences, v. 32, p. 151–185, doi: 10.1146/annurev.earth.32.101802.120356.

Whipple, K.X., and Tucker, G.E., 1999, Dynamics of the stream-power river incision model: Implications for height limits of mountain ranges, landscape response timescales, and research needs: Journal of Geophysical Research–Solid Earth, v. 104, p. 17,661–17,674, doi: 10.1029/1999JB900120.

Wobus, C., Whipple, K.X., Kirby, E., Snyder, N., Johnson, J., Spyropolou, K., Crosby, B., and Sheehan, D., 2006, Tectonics from topography: Procedures, promise and pitfalls, *in* Willett, S., Hovius, N., Brandon, M., and Fisher, D., eds., Tectonics, Climate, and Landscape Evolution: Geological Society of America Special Paper 398, p. 55–74, doi: 10.1130/2006.2398(04).

Wobus, C.W., Pringle, M.S., Whipple, K.X., and Hodges, K.V., 2008, A late Miocene acceleration of exhumation in the Himalayan Crystalline Core: Earth and Planetary Science Letters, v. 269, p. 1–10, doi: 10.1016/j.epsl.2008.02.019.

Xu, G.Q., and Kamp, P.J.J., 2000, Tectonics and denudation adjacent to the Xianshuihe fault, eastern Tibetan Plateau: Constraints from fission track thermochronology: Journal of Geophysical Research–Solid Earth, v. 105, p. 19,231–19,251, doi: 10.1029/2000JB900159.

York, D., 1968, Least-squares fitting of a straight line with correlated errors: Earth and Planetary Science Letters, v. 5, p. 320–324, doi: 10.1016/S0012-821X(68)80059-7.

Zeitler, P.K., 1985, Cooling history of the NW Himalaya, Pakistan: Tectonics, v. 4, p. 127–151, doi: 10.1029/TC004i001p00127.

Zeitler, P.K., Meltzer, A.S., Koons, P., Craw, D., Hallet, B., Chamberlain, C.P., Kidd, W., Park, S., Seeber, L., Bishop, M., and Shroder, J., 2001, Erosion, Himalayan geodynamics, and the geology of metamorphism: GSA Today, v. 11, no. 1, p. 4–8, doi: 10.1130/1052-5173(2001)011<0004:EHGATG>2.0.CO;2.

MANUSCRIPT RECEIVED 1 MAY 2009
REVISED MANUSCRIPT RECEIVED 17 NOVEMBER 2009
MANUSCRIPT ACCEPTED 17 NOVEMBER 2009

Printed in the USA